International Journal of Advance Research in Science and Engineering
Vol. No.10, Issue No. 03, March 2021
www.ijarse.com
IJARSE
ISSN 2319 - 8354

Study On Josephson vortex cores Regarding High-temperature Superconducting Junctions

[1]Ambuj Kumar, [2]Dr. Gajendra Prasad Gadkar,

[1]Research Scholar, Deptt. of Physics, Magadh University, Bodh Gaya

[2]Associate Professor, Department of Physics,

College of Commerce, Patliputra University

Abstract

This paper deals that when a normal metal is brought into contact with a superconductor, Cooper pairs may leak into the metal inducing genuine superconducting properties there, a phenomenon generically referred to as proximity effect[1]. If a normal metal is sandwiched between two superconductors, it can sustain the flow of dissipationless supercurrents[2]. When a magnetic field is applied across such a Josephson junction, the maximum of the supercurrent oscillates following a diffraction-like pattern[3], each oscillation corresponding to the entry of one Josephson vortex[4]. The on-demand generation and control of Josephson vortices is crucial for building advanced quantum devices such as coherent THz generators[5] or qubits for quantum computing[6]. In contrast to Abrikosov vortices in type II superconductors[7], the Josephson vortices are supposed to lack normal core and indeed, they have never been observed. Here, we report the direct imaging of Josephson vortices inside proximity junctions using scanning tunnelling microscopy. The Josephson vortex cores appear as regions where the proximity gap is locally suppressed and the normal state is recovered[8]. We demonstrate that the Josephson vortices are controlled by the edge supercurrents circulating in the superconducting leads. On the basis of our observation we suggest a novel method of generation and control of Josephson vortices by purely electrical means, which a crucial step toward designing densely integrated superconducting quantum devices.

Introduction

In 1963 Rowel[3] observed the oscillations of the critical current in superconducting junctions subject to a magnetic field. Since his pioneering discovery, the effect has been reported in numerous superconductor - normal metal - superconductor (SNS) weak links[4,9], including many examples in which the links were made of recently discovered materials like graphene[10] and topological insulators[11,12]. This macroscopic quantum interference effect is commonly interpreted as a sequence of Josephson vortices[4] penetrating the junction. By analogy with the Abrikosov vortices in type II superconductors[5], Josephson vortices were historically defined as regions with zero net circulating current and enclosing a magnetic flux quantum, . Yet, the spectral fingerprint of these quantum objects and their spatial organization remained till now undecided, and subject of controversy. The common wisdom is that Josephson vortices lack specific spectral signature and therefore cannot be identified. By contrast, recent microscopic calculations predicted that in diffusive SNS junctions Josephson vortices should be manifested as a spatial modulation of the proximity mini-gap in the quasiparticle excitation spectrum of the normal region of the junction[8]. Thus, Josephson vortices could probably have normal cores - regions where the proximity-gap vanishes, making possible their detection and imaging by e.g. scanning tunnelling microscopy, as is readily done for Abrikosov vortices in superconductors[13].

With this idea in mind, we created (see Methods) a lateral SNS network of superconducting Pb nanocrystals (in yellow in Fig. 1a) linked together by an atomically thin metallic (normal) Pb-wetting layer (appearing brown). The Pb-islands become superconducting below a critical temperature [18]. The local tunnelling conductance spectra measured on top of the superconducting islands at (see Methods) exhibit a superconducting gap (a typical spectrum S1 is presented in Fig. 1d). The wetting layer is non-superconducting, and the conductance spectra measured far from the islands show no superconducting gap but a tiny dip centred at the Fermi level (a typical spectrum WL is presented in Fig. 1d). This dip is a fingerprint of the Altshuler-Aronov zero-bias anomaly[19] due to electron-electron interaction in this two-dimensional diffusive metal[20]. Very close to the islands the superconducting correlations induce a small proximity gap in tunnelling spectra of the wetting layer (see curve PR in Fig. 1d). In the zero-bias conductance map in Fig. 1b the proximity gap appears as a bluish halo extending over a few tens of nanometres away from islands[20]. In locations where the edges of neighbouring islands get very close, this proximity halo becomes reinforced and appears in deeper blue. The phenomenon reflects the overlap of superconducting correlations induced by both islands[21,22], that enhances the proximity gap (Fig. 1d). This results in the formation of SNS Josephson junctions, as those seen in locations J1-J4.

We now follow the evolution of the proximity links in applied magnetic field. The spectroscopic map acquired at shows the usual penetration of Abrikosov vortices in the large islands, while the small ones remain in the vortex-free Meissner state[18] (Fig. 1c). By contrast, unusual features are revealed in proximity links inside the SNS junctions, and identified as Josephson vortices. Precisely, while at zero field the proximity gap is observed in all three locations A, B, C of the junction J1 (Fig. 1e), at no proximity gap is observed in B (Fig. 1f), but instead a normal state with its Altshuler-Aronov zero-bias dip is recovered. In the neighbouring positions A and C however, the proximity gap persists (Fig. 1e & f). This behaviour is confirmed by the conductance map in Fig. 1c where two clear Josephson links remain at in locations A and C (in blue), while in B the proximity gap vanishes (high conductance, in yellow-red). The normal region in B surrounded by gapped areas is thus indeed a Josephson vortex core. The spectroscopic maps in Fig. 2a & b focus on junctions J2-J4 located in the framed part of Fig. 1a. They show how Josephson vortex configurations change with magnetic field. Both J2 and J3 junctions accept one Josephson vortex at (Fig. 2a) and two at (Fig. 2b). The very short and narrow junction J4 does not accept any Josephson vortex in its centre up to , but it is visually suggestive that one vortex is about to appear on the left side of J4. In all studied SNS junctions, Josephson vortex cores are in the normal state, as predicted[8].

The interpretation of our observation in terms of Josephson vortex cores is fully corroborated by numerical simulations in Fig. 2c & d; the calculation method is described in Fig. We first calculated the Abrikosov vortex configurations in islands using Ginzburg-Landau formalism (see S1). As an example, in Fig. 3a the Cooper-pair density map calculated at reproduces the experimentally observed Abrikosov vortex configuration (Fig. 1c). In Fig. 3b the corresponding phase portrait of the superconducting order parameter shows that the interplay between Meissner and vortex currents results in a spatially evolving phase inside islands. At this point, the physical origin of Josephson vortices is revealed, considering the gauge-invariant local phase difference across the junction, , where are local phases of the order parameter at two island edges at positions (on opposite sides of a given junction) and is the vector potential. At locations in which Is , the superconducting correlations induced by both islands are in phase, their constructive interference resulting in a well-developed proximity gap. On the contrary, in locations where is the superconducting correlations induced by both islands interfere destructively and the proximity gap is suppressed[24]. This situation corresponds to Josephson vortex cores.

Using we find a current circulating around Josephson vortices. As a rough approximation, the Josephson current can be considered locally as simply proportional to . In the junction J1, for instance, in locations between A and B, varies continuously from to , and some net Josephson current flows locally from one island edge to the other one. In the opposite case, from B to C the phase difference varies continuously from to , , and the current flows in the opposite direction. Therefore, Josephson current circulates around the point B, thus justifying the term 'Josephson vortex'. The above phase considerations served as a basis for numerical simulations. Starting from the phase portrait of Fig. 3b we calculated, for each location inside the junctions, the strength of the superconducting correlations as interference between two evanescent waves having a phase difference (see S2). The result of these calculations is displayed in Fig. 3c, ideally reproducing the experimentally observed position and extent of the Josephson vortex in the junction J1 (Fig. 1c). In the same manner the correlation maps in Fig. 2c & d were calculated, matching again the experimental findings (Fig. 2a & b). The success of our method in simulating Josephson vortices clearly highlights that the Josephson vortices in our system originate from nothing but quantum interference.

Next, we calculated the spatial evolution of the density of states inside the Josephson vortex core, which cannot be obtained from correlation maps, but which we derived using the Usadel microscopic approach[8,25] (see S3). Fig. 4a shows the calculated map of the local density of states

International Journal of Advance Research in Science and Engineering
Vol. No.10, Issue No. 03, March 2021
www.ijarse.com
IJARSE
ISSN 2319 - 8354

at the Fermi energy for a junction similar to J1. The map demonstrates the suppression of the proximity gap inside Josephson vortex cores[8]. This suppression is further detailed in Fig. 4b where we show the local density of states as a function of energy at various distances from the centre of a vortex. Using these results we generated the corresponding tunnelling conductance spectra (Fig. 4c). In this calculation the Altshuler-Aronov zero-bias effect was taken into account[20]. As one can see, the Usadel approach reproduces qualitatively the observed vanishing of the proximity gap in Figs. 1e & f.

In the present study, the gauge-invariant phase difference that generates Josephson vortices was created with the help of an applied magnetic field. Equivalently, the gauge-invariant phase differences may be generated by edge supercurrents circulating in S-electrodes. Indeed, in zero

magnetic field, taking the gauge , we get a simple current-phase expression, ,

where is the effective coherence length, and is the critical current in the electrode, . Therefore, if the superconducting electrodes of the junction carry oppositely directed currents along the electrode edge, a gauge-invariant phase difference appears across the junction. It evolves with the lateral position inside the junction as , leading to formation of Josephson vortex. To confirm this idea, we carried out calculations of the local density of states in SNS junctions where currents flow inside S-leads along the junction edges but there is no applied magnetic field (see S3 for details). We show in Fig. 4d a typical result for a junction similar to J2, where we have assumed that opposite currents circulate along both interface edges.

As one can see, there appear Josephson vortices with normal cores, very similar to those induced magnetically (see Fig. 4a). In this case, the density and size of generated Josephson vortices is simply proportional to the intensity of circulating edge currents. Moreover, vortex generation may also be achieved if only one superconducting lead carries a supercurrent, as we demonstrate in Fig. 4e. By tuning intensities of supercurrents in leads one may pin vortices at one or other edge. In a SNS device, like the one sketched in Fig. 4f, it should be possible to create Josephson vortices by simply applying currents through superconducting leads. Such a method would open new pathways for generation and control of quantum objects by purely electrical means, without the need of any externally applied magnetic field.

Methods Summary

The 7×7 reconstructed n-Si(111) ($n \approx 10^{19}$ cm^{-3}) was prepared by direct current heating to 1200°C followed by annealing procedure between 900°C and 500°C. Subsequently, few atomic layers of Pb were evaporated on the Si(111)-7×7 kept at room temperature, using an electron beam evaporator calibrated with a quartz micro-balance. The resulted flat top (111) oriented single nano-crystal of Pb are interconnected via disordered atomic wetting layer of Pb[16,17, 20]. At any stage of the sample preparation the pressure did not exceed $P = 3\times10^{-10}$ mbar. The sample structure was controlled in both real and reciprocal space by scanning tunnelling microscopy and Low Energy Electron Diffraction.

The scanning tunnelling spectroscopy measurements were performed in situ with a homemade apparatus, at a base temperature of and in ultrahigh vacuum $P < 3 \times 10^{-11}$ mbar; the electron temperature was estimated to be . Mechanically sharpened Pt/Ir tips were used.

The bias voltage was applied to the sample with respect to the tip. Typical set-point parameters for spectroscopy are at . The tunneling conductance curves *dI(V)/dV* were numerically derivated from raw *I(V)* experimental data. Each conductance map is extracted from a set of data consisting of spectroscopic *I(V)* curves measured at each point of a 512x512 grid, acquired simultaneously with the topographic image. The magnetic field was applied perpendicular to the sample surface.

The frameworks for the theoretical simulations in this paper are the phenomenological Ginzburg-Landau (GL) theory[4] and microscopic Usadel modelisation[8,25]. The GL simulations were implemented on a Cartesian grid for the exact geometry of the islands and expected electron mean-free path in the samples (see S1), using STM mapping from the experiment, with grid spacing of 1 nm. The equations were solved self-consistently in 3D and contain higher order derivatives; for this demanding computation we have used GPU parallel computing. The

International Journal of Advance Research in Science and Engineering
Vol. No.10, Issue No. 03, March 2021
www.ijarse.com
IJARSE
ISSN 2319 - 8354

description of the local density of states and tunnelling spectra of the SNS junctions was carried out using the Usadel approach as explained in detail in S3 of the Supplementary Information.

References:

1 de Gennes, P. G. Boundary effects in superconductors. *Rev. Mod. Phys.* 36, 225 (1964).

2 Josephson, B. D. Possible new effects in superconductive tunnelling, *Phys. Lett.* 1, 251 (1962).

3 Rowell, J. M. Magnetic field dependence of the Josephson tunnel current. *Phys. Rev. Lett.* 11, 200 (1963).

4 Tinkham, M. *Introduction to Superconductivity* (McGraw Hill, New York, 1996).

5 Ulrich Welp, U., Kadowaki K., and Kleiner, R. Superconducting emitters of THz radiation. *Nature Photonics* 7, 702–710 (2013), and refs. 18-25 therein

6 Devoret, M. et al. Macroscopic quantum effects in the current-biased Josephson junction in *"Quantum Tunneling in Condensed Media", edited by Y. Kagan, and A.J. Leggett*. (Elsevier Science Publishers,1992) pp. 313-345; Devoret, M., and Schoelkopf, R. Superconducting Circuits for Quantum Information: An Outlook. *Science* 339, 6124, 1169-1174 (2013)

7 Abrikosov, A. A. On the magnetic properties of superconductors of the second group. *Sov. Phys. JETP* 5, 1174 (1957).

8 Cuevas, J. C. & Bergeret, F. S. Magnetic interference patterns and vortices in diffusive SNS junctions. *Phys. Rev. Lett.* 99, 217002 (2007).

9 Barone, A. & Paterno, G. *Physics and Applications of the Josephson Effect* (Wiley, New York, 1982).

10 Heersche, H. B., Jarrillo-Herrero, P., Oostinga, O. O., Vandersypen, L. M. K. & Morpurgo, A. F. Bipolar supercurrent in graphene. *Nature* 446, 56 (2007).

11 Veldhorst, M. *et al.* Josephson supercurrent through a topological insulator surface state. *Nature Mat.* 11, 417 (2012).

12 Williams, J. R. *et al.* Unconventional Josephson effect in hybrid superconductor-topological insulator devices. *Phys. Rev. Lett.* 109, 056803 (2012).

13 Hess, H. F., Robinson, R. B., Dynes, R. C., Valles, J. M. & Waszczak, J. V. Scanning-tunneling-microscope observation of the Abrikosov flux lattice and the density of states near and inside a fluxoid. *Phys. Rev. Lett.* 62, 214 (1989).

14 Eom, D. Qin, S. Chou, M.-Y. & Shih, C. K. Persistent superconductivity in ultrathin Pb films: a scanning tunneling spectroscopy study. Phys. Rev. Lett. 96, 027005 (2006).

15 Nishio, T. *et al.*, Superconducting Pb Island Nanostructures Studied by Scanning Tunneling Microscopy and Spectroscopy. *Phys. Rev. Lett.* 101, 167001 (2008).

16 Cren, T., Fokin, D., Debontridder, F. Dubost, F. & Roditchev, D. *Phys. Rev. Lett.* 102, 127005 (2009).

17 Brun, C. *et al.* Reduction of the superconducting gap of ultrathin Pb islands grown on Si(111). *Phys. Rev. Lett.* 102, 207002 (2009).

18 Cren, T., Serrier-Garcia, L., Debontridder, F. & Roditchev, D. Vortex fusion and giant vortex states in confined superconducting condensates. *Phys. Rev. Lett.* 107, 097202 (2011).

19 Altshuler, B. L. & Aronov, A. G. in Electron-Electron Interactions in Disordered Systems, edited by A. L. Efros and M. Pollak (Elsevier Science Publisher B. V., Amsterdam, 1985).

20 Serrier-Garcia, L. *et al.* Scanning tunneling spectroscopy study of the proximity effect in a disordered two-dimensional metal. *Phys. Rev. Lett.* 110, 157003 (2013).

21 Golubov, A. A. & Kupriyanov, M. Yu. Theoretical investigation of Josephson tunnel junctions with spatially inhomogeneous superconducting electrodes. *J. Low Temp. Phys.* 70, 83 (1988).

22 Belzig, W. *et al.*, Local density of states in a dirty normal metal connected to a superconductor. *Phys. Rev. B* 54, 9443 (1996).

23 Kim, J., Chua, V., Fiete, G. A., Nam, H., MacDonald, A. H. & Shih, C.-K. Visualization of geometric influences on proximity effects in heterogeneous superconductor thin films. *Nat. Phys.* 8, 464 (2012).

24 le Sueur, H., Joyez, P., Pothier, H., Urbina, C. & Esteve, D. Phase controlled superconducting proximity effect probed by tunneling spectroscopy. *Phys. Rev. Lett.* 100, 197002 (2008).

International Journal of Advance Research in Science and Engineering
Vol. No.10, Issue No. 03, March 2021
www.ijarse.com
IJARSE
ISSN 2319 - 8354

25 Usadel, K.D. Generalized diffusion equation for superconducting alloys. *Phys. Rev. Lett.* 25, 507 (1970).

FIGURES

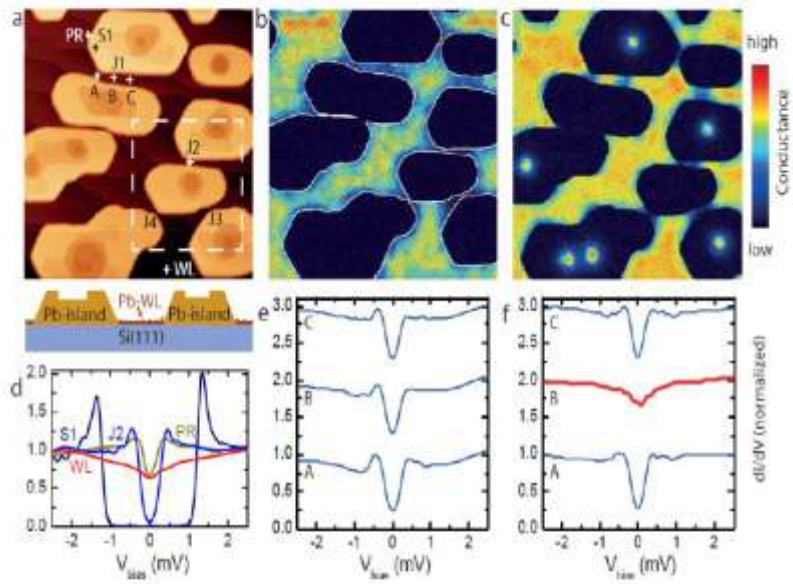

Figure 1 | Josephson vortices imaged by scanning tunnelling spectroscopy at 0.3 K. a

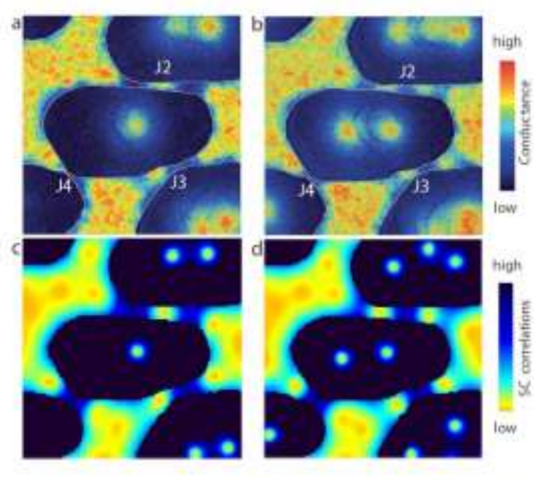

Figure 2 | Josephson vortex formation and evolution wih magnetic field. a

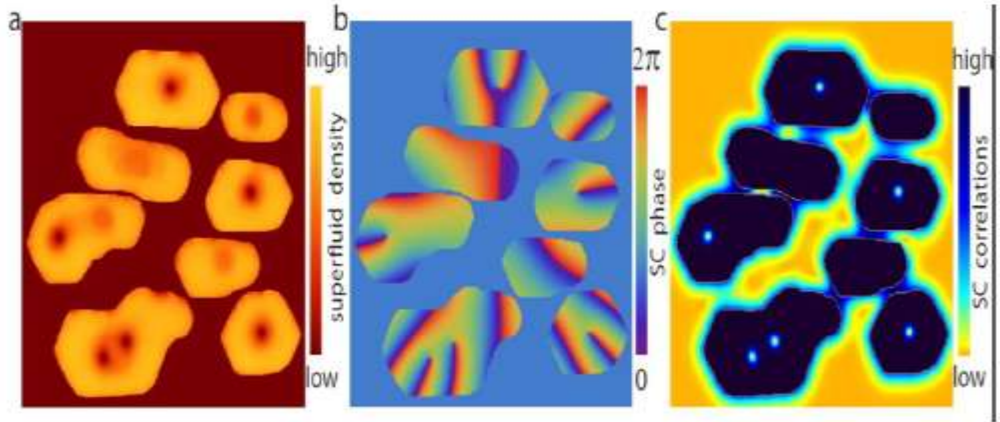

Figure 3 | Simulation of Josephson vortex maps. a 1000nm x 1000nm colour-coded spatial

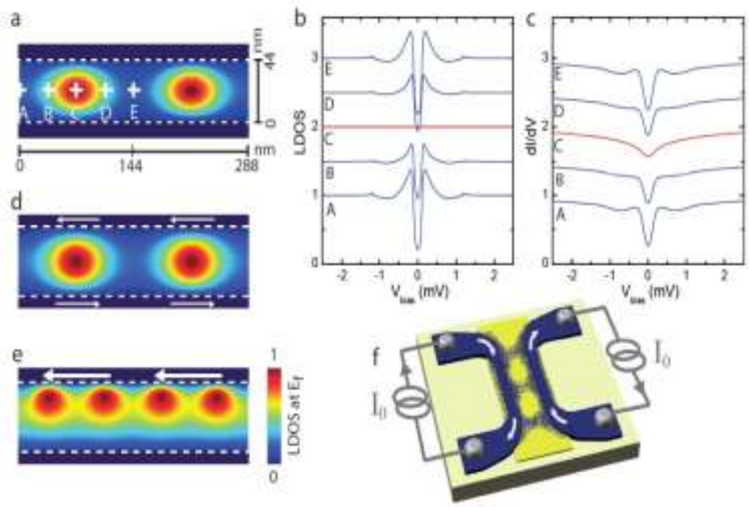

Figure 4 | Josephson vortex core: density of states and principle of generation by edge